Experimental and theoretical studies on the corrosion inhibition potentials of *N′*-((1*H*-indole-3-yl)methylene)benzohydrazide for mild steel in HCl

J.A. Ibrahim,[1]* H.H. Ibraheem[1] and H.T. Hussein[2]

[1]*University of Technology (UOT), Department of Applied Science, Branch of Applied Chemistry, 8C6W+6P2, Al Senaha St, Baghdad, Baghdad Governorate, Iraq*
[2]*University of Technology (UOT), Department of Applied Science, Physics Division, 8C6W+6P2, Al Senaha St, Baghdad, Baghdad Governorate, Iraq*
**E-mail: as.21.40@grad.uotechnology.edu.iq*

Abstract

In this study, we introduce a novel corrosion inhibitor, *N′*-((1*H*-indole-3-yl)methylene)benzohydrazide (IMBH) synthesized from indole-3-carboxyaldehyde. The inhibitory properties of IMBH and the starting material were investigated for mild steel in hydrochloric acid (HCl) solutions of varying concentrations (0.2 M, 0.4 M, and 0.6 M). The evaluation of corrosion inhibition was performed using a combination of scanning electron microscopy (SEM), energy dispersion X-ray analysis (EDX) techniques, and electrochemical measurements. Our findings demonstrate a clear correlation between the concentration of the inhibitor and its inhibition effectiveness. As the concentration of IMBH rises, the corrosion of mild steel is more effectively controlled. The inhibition mechanism mainly operates through a charge transfer process, where the formation of protective adsorption layers on the steel surface plays a significant role in mitigating corrosion. Furthermore, we employed quantum chemical calculations to gain insights into the inhibitory process, offering valuable theoretical support for our experimental observations. This investigation sheds light on the promising corrosion inhibition potential of IMBH and its feasibility as a protective agent for mild steel in acidic environments. The understanding of its inhibitory mechanism, facilitated by quantum chemical analysis, provides essential knowledge for the development of effective corrosion prevention strategies in various industrial applications.

Received: July 28, 2023 Published: January 15, 2024 doi: 10.17675/2305-6894-2024-13-1-6

Keywords: *scanning electron microscopy, energy dispersion X-ray analysis, charge transfer, protective adsorption layers, quantum chemical calculations.*

Introduction

Mild steel, commonly known as low-carbon steel, holds significant importance in various industrial applications due to its cost-effectiveness and versatility. It finds widespread usage in chemical and related sectors, particularly in handling acid, alkali, and salt solutions [1, 2]. However, the susceptibility of mild steel to corrosion poses a significant challenge in

maintaining its structural integrity and longevity [3–8]. Corrosion, a complex chemical process involving the interaction of ions with metal surfaces, is a result of metal deterioration caused by exposure to the environment. To combat the detrimental effects of corrosion, employing effective corrosion control methods becomes imperative. Organic inhibitors have proven to be successful in mitigating corrosion-related issues [9–17]. The inhibitory performance of an organic compound depends on its chemical composition, the metal surface's charge, and the interactions between the organic molecule and the metal surface, primarily through surface adsorption [18–23]. Schiff bases, characterized by an azomethine bond (C=N), exhibit diverse applications in research, ranging from corrosion inhibition to therapeutic uses. These compounds possess heteroatoms that play a crucial role in inhibiting corrosion on metal surfaces, particularly in acidic environments [24, 25]. Some studies have highlighted the superior inhibitory abilities of Schiff bases compared to similar amines and aldehydes, attributed to the presence of a –C=N– group in the molecule [26–28]. The primary aim of this study is to investigate the corrosion inhibition potential of a newly synthesized Schiff base, *N*′-((1*H*-indole-3-yl)methylene)benzohydrazide (IMBH), obtained through the condensation of indole-3-carboxaldehyde with benzohydrazide (BH). The inhibitory properties of IMBH will be explored for mild steel in HCl solutions. The study aims to assess the factors influencing the corrosion inhibition efficiency, such as inhibitor concentration, temperature, and exposure time. The novelty of this work lies in the chemical synthesis and characterization of the novel Schiff base, IMBH, and its exploration as a corrosion inhibitor for mild steel. By focusing on the unique azomethine bond (C=N) present in Schiff bases, this study aims to shed light on the potential advantages of IMBH over conventional inhibitors.

The objectives of the current study are:

1. Synthesis and characterization of IMBH as a novel Schiff base inhibitor using proton nuclear magnetic resonance (^{1}H NMR), carbon-nuclear magnetic resonance (^{13}C NMR), Fourier transform infrared spectroscopy (FT-IR), and CHN elemental analysis.
2. Evaluation of the corrosion inhibition performance of IMBH for mild steel in hydrochloric acid (HCl) solutions and comparison with other Schiff base inhibitors.
3. Investigation of key influencing factors, such as inhibitor concentration, temperature, and exposure time, on the corrosion inhibition efficiency of IMBH.
4. Utilization of electrochemical and scanning electron microscopy techniques to assess the inhibitive performance and the surface morphology of the mild steel samples exposed to IMBH as a corrosion inhibitor.

Experimental

Chemistry

The initial components and solvents for the experiments were obtained from Sigma Aldrich Chemical Co. and Fluka. To create the corrosive hydrochloric acid solutions of varying concentrations (0.2 M, 0.4 M and 0.6 M), double-distilled water was used for dilution. The corrosion inhibitor, IMBH, was synthesized and then prepared in different concentrations (0.0005 M, 0.001 M, and 0.005 M) and added to the corrosive environments. The proton and carbon-13 nuclear magnetic resonance spectra were recorded using an AVANCE III 600 MHz Bruker spectrometer (Billerica, MA, USA) with dimethylsulfoxide as the solvent. Fourier Transform Infrared (FT-IR) spectra were obtained using a Thermo Nicolet Corp. 6700 FTIR Nicolet spectrophotometer (Madison, WI, USA). The progress of the reaction was monitored using thin-layer chromatography (TLC) with silica gel 60 plates [29, 30].

Synthesis of IMBH

The synthesis of IMBH involved the following steps.

Preparation of BH

A 1:1 mixture of ethyl benzoate (4.505 g, 0.03 mol) and hydrazine hydrate (0.96 g, 0.03 mol) in an ethanolic solution was refluxed for 6 hours. The resulting white precipitate was filtered, washed with cold ethanol multiple times, and vacuum-dried to obtain the hydrazide derivative which recrystallized from ethanol with a yield of 85%. Melting Point (MP): 112–114°C. FT-IR: 3298 cm^{-1}, 3219 cm^{-1}, and 3205 cm^{-1} (NH and NH_2 stretching); 1658 cm^{-1} (C=O stretching); 3018 cm^{-1} (Ar–H stretching).

Synthesis of IMBH

A solution containing 1.36 g (0.01 mol) of the hydrazide derivative BH, 25 mL of pure ethanol, and 0.01 mol of indole-3-carboxaldehyde was refluxed with a few drops of glacial acetic acid for four hours. The resulting yellow precipitate was filtered, washed with ethanol, and vacuum-dried to obtain the Schiff base (recrystallized from ethanol) with a yield of 80%. MP: 239–241°C. FT-IR: 3209 cm^{-1} (NH stretching); 1608 cm^{-1} (C=N stretching); 3039 cm^{-1} (Ar–H stretching); 1573 cm^{-1}, 1442 cm^{-1} (C=C stretching). The chemical structure of the synthesized molecule was confirmed using proton nuclear magnetic resonance (^{1}H NMR) spectroscopy. ^{1}H NMR in ppm: 11.64 (s, 1H, –NH indole); 11.54 (s, 1H, =N–NH–); 8.63 (s, 1H, –N=CH); 7.15 (m, 10H, Ar–H). Carbon-13 nuclear magnetic resonance (^{13}C NMR) was also performed to identify carbon atoms in the synthesized molecules. ^{13}C NMR in ppm: 112.20; 112.28; 120.85; 122.51; 123.10; 124.83; 127.94; 128.87; 130.79; 131.78; 134.55; 137.51; 145.41; 162.97.

Specimens and solution

Square specimens of mild steel were prepared from commercially available mild steel rods with the following chemical composition (wt.%): Si (0.83%), Fe (91.56%), C (1.42%), Al (0.12%), Mn (1.26%), Cu (0.10%), Cr (1.72%), Mg (0.02%). The coupons dimensions were 1 cm×1 cm×0.3 cm. The mild steel samples were thoroughly cleaned following the ASTM standard procedure G1-03 [28]. All experiments were conducted using hydrochloric acid prepared by diluting 37 percent HCl in water [30].

Electrochemical measurement

Before initiating the electrochemical measurements, open circuit potentials for various acidic electrolytes (0.2 M, 0.4 M and 0.6 M) were determined. The mild steel samples were immersed in the electrolyte for 15 minutes, and then the open circuit potentials were recorded over a 30-minute period. Tafel measurements were performed using the potentiodynamic mode in the electrolytes for the mild steel specimens. A standard three-electrode cell setup was used, with a saturated calomel electrode (SCE) as the reference electrode, a platinum plate as the counter electrode, and the samples as the working electrode. The potential was scanned from a negative value to the previously measured open circuit potential (OCP) and then positive to achieve polarization. The potential range was from –250 mV to +250 mV *vs* OCP, and the scan rate was set at 1 mV/s. Electrochemical measurements were carried out using the CS 310 CorrTest workstation from Wuhan, China. Equations 1 and 2 were used to calculate the inhibition performance.

$$IE\% = \frac{C_{\mathrm{R}} - C_{\mathrm{Ri}}}{C_{\mathrm{R}}} \cdot 100 \tag{1}$$

$$C_{\mathrm{R}} = \frac{C_{\mathrm{R}} - C_{\mathrm{Ri}}}{C_{\mathrm{R}}} \tag{2}$$

where C_{Ri} is the corrosion rate measured while the tested inhibitor is present, and C_{R} is the corrosion rate measured in the absence of the tested inhibitor.

Surface analysis

To analyze the changes in the metal surface after immersion in 0.2 M HCl with and without IMBH and the starting material indole-3-carboxaldehyde, SEM and EDX were employed.

Theoretical study

Theoretical calculations and optimized geometries of the inhibitors indole-3-carboxaldehyde and IMBH were carried out using the Gaussian 09 program, version D.01, at the DFT-B3LYP level with the basis set 6-311G. Additionally, the highest and lowest molecular orbital energies, E_{HOMO} and E_{LUMO}, respectively, were used to gain insight into the inhibitory behavior [32, 33].

Results and Discussion

Chemistry

Schiff bases (SBs) represent a vital class of chemical compounds with diverse applications in both biology and industry. These compounds are typically denoted as $R_1R_2C{=}NR_3$ ($R_3{-}H$), where the aryl or alkyl substituent at position $-R_3$ distinguishes SBs as a subclass of imines. The groups R_1 and/or R_2 can also be hydrogen. In the present study, the Schiff base IMBH was synthesized through the condensation of BH and indole-3-carboxaldehyde, as illustrated in Scheme 1.

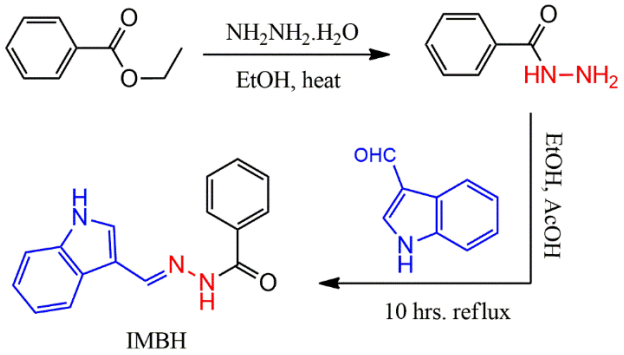

Scheme 1. Chemical synthesis of IMBH from BH and indole-3-carboxaldehyde.

The chemical structure and spectral data of the synthesized Schiff base IMBH were determined using various spectroscopic techniques. The Fourier Transform Infrared (FT-IR) spectrum as in Figure 1, displayed characteristic peaks at 3209 cm^{-1} (NH stretching), 1608 cm^{-1} (C=N stretching), 3039 cm^{-1} (Ar–H stretching), and 1573 cm^{-1} and 1442 cm^{-1} (C=C stretching).

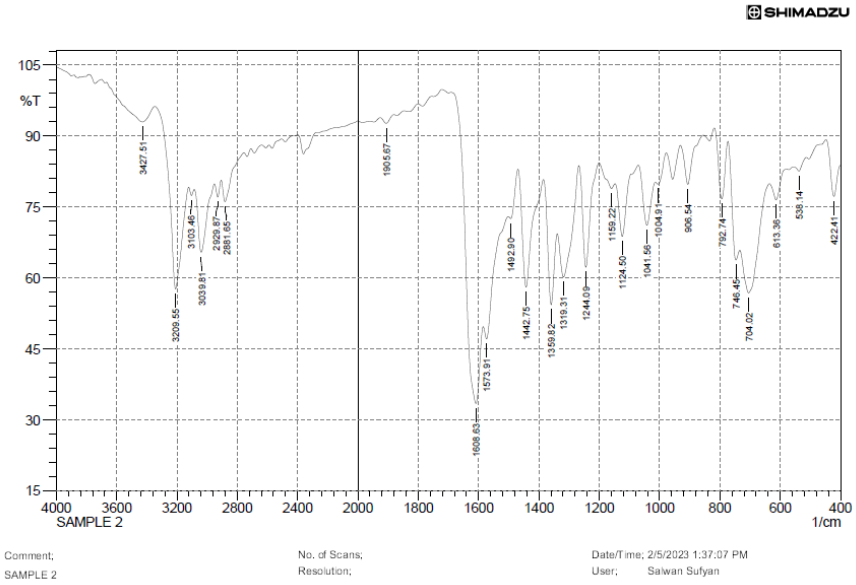

Figure 1. FT-IR curve of IMBH.

The proton nuclear magnetic resonance (^{1}H NMR) spectroscopy as in Figure 2, provided valuable insights into the hydrogen-1 nuclei, indicating peaks at 11.64 ppm (singlet, ^{1}H, –NH indole), 11.54 ppm (singlet, ^{1}H, =N–NH–), 8.63 ppm (singlet, ^{1}H, –N=CH), and 7.15 ppm (multiplet, 10H, Ar–H).

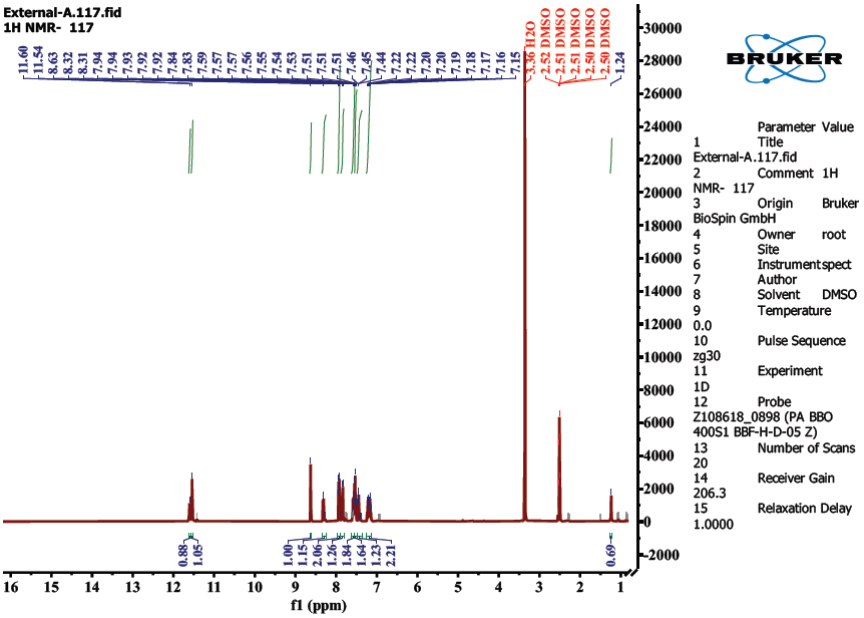

Figure 2. ^{1}H NMR spectra of IMBH.

Additionally, the carbon-13 nuclear magnetic resonance ^{13}C NMR spectroscopy as in Figure 3, further confirmed the chemical structure, revealing peaks at various chemical shifts, including: 112.20; 112.28; 120.85; 122.51; 123.10; 124.83; 127.94; 128.87; 130.79; 131.78; 134.55; 137.51; 145.41 and 162.97 ppm.

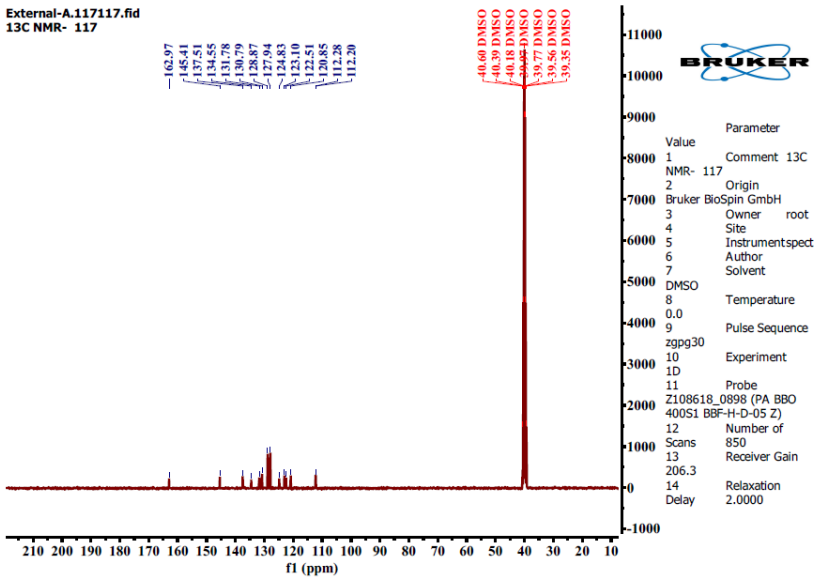

Figure 3. ^{13}C NMR spectra of IMBH.

The successful synthesis of IMBH was confirmed by these spectroscopic data and physical characteristics (Table 1), corroborating the formation of the desired Schiff base. The yield of the Schiff base IMBH was found to be 80%, indicating the efficiency of the condensation reaction. The newly synthesized Schiff base IMBH exhibited unique structural features attributed to the presence of the azomethine bond (C=N) and aromatic moieties, which are vital for its potential as a corrosion inhibitor. The presence of nitrogen and carbon atoms in the structure suggests potential sites for the formation of coordination complexes with the metal surface, thereby facilitating corrosion inhibition. The Schiff base IMBH derived from the condensation of BH and indole-3-carboxaldehyde holds promise as an effective corrosion inhibitor due to the presence of functional groups known for their ability to form protective adsorption layers on metal surfaces. Further investigation of the corrosion inhibition performance of IMBH for mild steel in HCl solutions will provide crucial insights into its practical application as a corrosion control agent. The spectroscopic data obtained in this study serve as a foundation for understanding the inhibitory mechanism and structure-activity relationship of IMBH as a potential corrosion inhibitor.

Table 1. Physical data of Schiff base.

Compound	M.P, °C	Color	Yield, %	Molecular formula	R_f
IMBH	239–241	Off white	80%	$C_{16}H_{13}N_3O$	0.7

Electrochemical studies

The corrosion behavior of the investigated mild steel (MS) samples in HCl solutions with different concentrations of the inhibitors, indole-3-carboxyaldehyde and IMBH, was evaluated using Tafel measurements. The results are summarized in Table 2.

The addition of the inhibitors indole-3-carboxyaldehyde and IMBH led to a significant improvement in the inhibition efficiency (*IE*), as in Figures 4, 5 and 6, indicating their potential as effective corrosion inhibitors for mild steel. The enhanced inhibitory effect can be attributed to the formation of an inhibitor layer on the metal surface, which acts as a protective barrier, reducing the corrosion rate [34–39]. The presence of heteroatoms, particularly the –C=N– group, in indole-3-carboxyaldehyde and IMBH facilitated strong adsorption on the mild steel surface, contributing to the formation of this protective layer. As the concentration of indole-3-carboxyaldehyde and IMBH increased, a higher degree of adsorption occurred on the mild steel surface, leading to the formation of a thicker and more effective protective layer. This is reflected in the increasing *IE* as the inhibitor concentration rises. The comparison between indole-3-carboxyaldehyde and IMBH revealed that IMBH exhibited higher inhibitory potency. This can be attributed to the presence of additional adsorption centers, including the –C=N– group and the heterocyclic group, in the molecular structure of IMBH. These features provide more active sites for interaction with the metal surface, resulting in enhanced protection against corrosion [40–44]. The data presented in

Table 2 clearly demonstrate the corrosion rates (C_R) and inhibition efficiencies (%) determined by electrochemical analyses for mild steel samples immersed in hydrochloric acid solutions of varying concentrations (0.2 M, 0.4 M, and 0.6 M) containing different concentrations of indole-3-carboxyaldehyde and IMBH.

Table 2. Corrosion rates (C_R) and inhibition efficiencies (%) for mild steel in hydrochloric acid solutions with varying inhibitor concentrations.

Compound	Concentration	C_R (g/cm^{-}2·day^{-1})	θ	*IE* %
Blank	0.2	1.074	–	–
Indole-3-carboxyaldehyde	0.0005	0.989	0.008	8.000
	0.001	0.322	0.700	70.00
	0.005	0.214	0.800	80.00
IMBH	0.0005	0.849	0.210	21.00
	0.001	0.209	0.805	80.500
	0.005	0.001	0.990	99.85
Blank	0.4	1.211	–	–
Indole-3-carboxyaldehyde	0.0005	1.119	0.070	7.60
	0.001	0.544	0.550	55.06
	0.005	0.363	0.700	70.02
IMBH	0.0005	0.964	0.204	20.40
	0.001	0.336	0.722	72.20
	0.005	0.027	0.977	97.70
Blank	0.6	1.449	–	–
Indole-3-carboxyaldehyde	0.0005	1.348	0.070	7.00
	0.001	0.694	0.520	52.07
	0.005	0.543	0.625	62.53
IMBH	0.0005	1.168	0.194	19.43
	0.001	0.449	0.690	69.00%
	0.005	0.063	0.956	95.60

The results in Table 2 illustrate that in the absence of any inhibitor (Blank), the corrosion rates for mild steel were relatively high, indicating a significant corrosion propensity. However, upon the addition of indole-3-carboxyaldehyde and IMBH, the corrosion rates decreased substantially, and the inhibition efficiencies showed a remarkable improvement. For instance, in 0.4 M HCl solution, at a concentration of 0.001 M, indole-3-

carboxyaldehyde demonstrated an inhibition efficiency of 55.06%, while IMBH at the same concentration exhibited an impressive inhibition efficiency of 72.2% [45–51]. Moreover, at a higher concentration of 0.005 M, IMBH exhibited an outstanding inhibition efficiency of 97.7% compared to 70.02% for indole-3-carboxyaldehyde. This clearly highlights the superior inhibitory performance of IMBH over indole-3-carboxyaldehyde in this corrosive environment. These electrochemical studies provide crucial insights into the effectiveness of indole-3-carboxyaldehyde and IMBH as corrosion inhibitors for mild steel in hydrochloric acid solutions. The results underscore the potential of IMBH as a promising corrosion control agent, thanks to its unique molecular structure and higher adsorption capabilities, making it an attractive candidate for practical industrial applications.

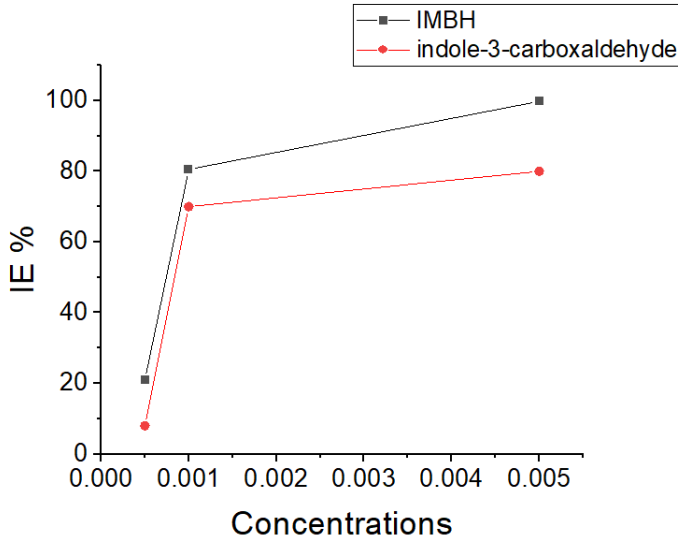

Figure 4. Impact of indole-3-carboxaldehyde and IMBH concentration on inhibition efficiency at 0.2 M HCl of mild steel.

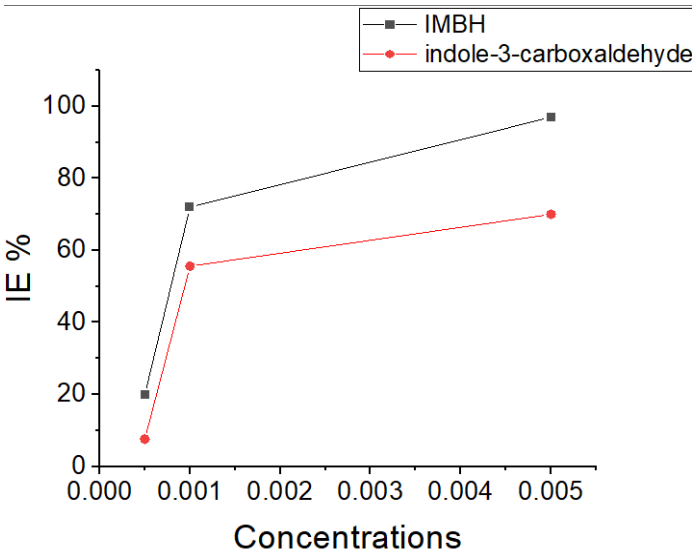

Figure 5. Impact of indole-3-carboxaldehyde and IMBH concentration on inhibition efficiency at 0.4 M HCl of mild steel.

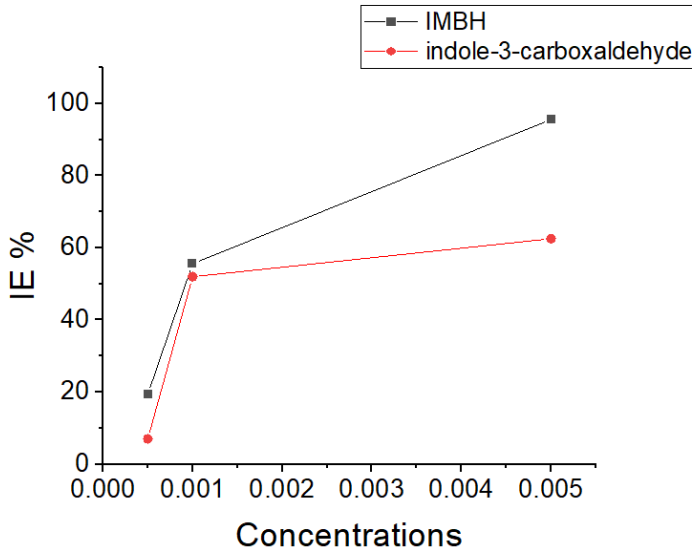

Figure 6. Impact of indole-3-carboxaldehyde and IMBH concentration on inhibition efficiency at 0.6 M HCl of mild steel.

Surface analysis

The surface analysis of the mild steel samples provided valuable insights into the corrosion inhibition mechanism facilitated by the adsorption of the inhibitors. To illustrate the experimental findings, SEM images of the mild steel surface were acquired in a 0.2 M HCl solution, both in the absence and presence of the tested inhibitor at a concentration of 0.005 M. Figure 7 showcases the SEM images.

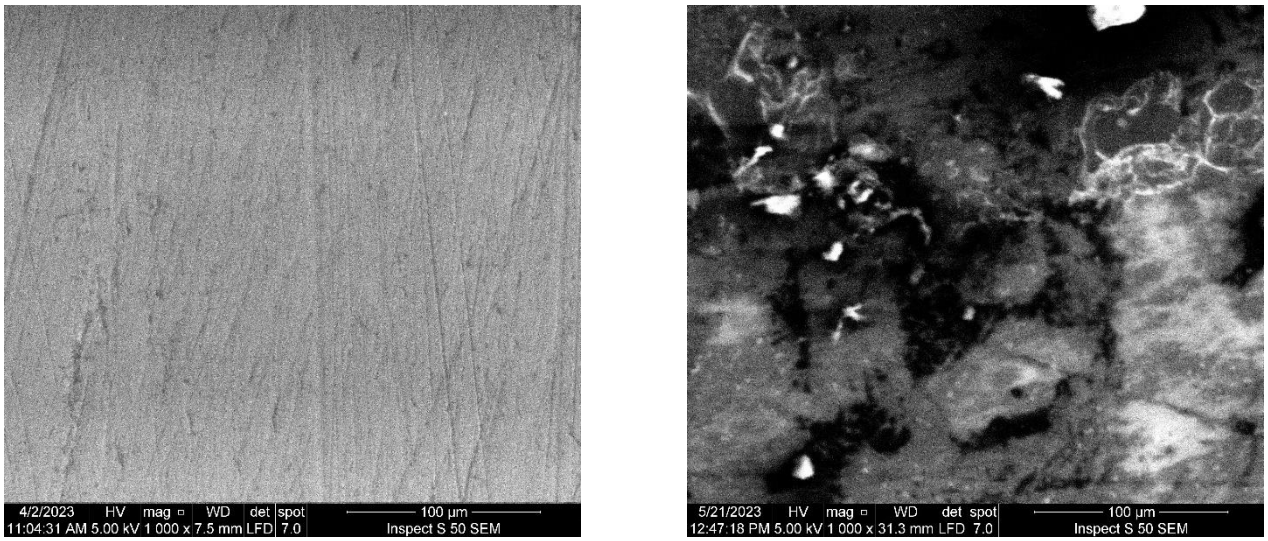

(A) (B)

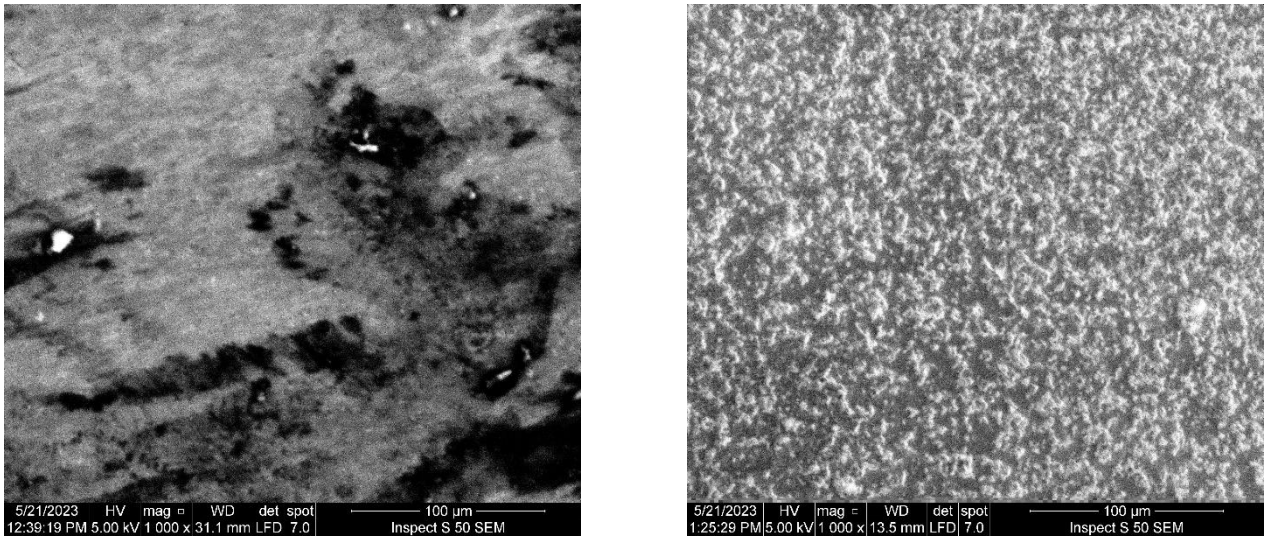

(C) (D)

Figure 7. SEM images of mild steel surface. (A) polished surface, (B) after immersion in 0.2 M HCl, (C) after immersion in 0.2 M HCl, 0.005 M of indole-3-carboxyaldehyde, (D) after immersion in 0.2 M HCl, 0.005 M of IMBH.

Figure 7 (a) illustrates the impact of corrosion conditions on the mild steel surface without the presence of the tested inhibitor. The SEM image clearly reveals the formation of pits on the surface, indicative of the aggressive attack by the 0.2 M hydrochloric acid medium. These pits are characteristic of the corrosive nature of the acidic environment. (b) In contrast, Figure 7 (b) shows the mild steel surface in the presence of the tested inhibitor at a concentration of 0.005 M. The addition of the inhibitor significantly reduced the rate of corrosion, leading to a visibly altered metal surface morphology. The SEM image demonstrates the formation of a protective layer of inhibitor molecules on the mild steel surface. This adsorbed layer acts as a barrier, shielding the metal from direct contact with the corrosive medium and hindering the corrosion process. Figure 7 (c) and (d) provide crucial information concerning the effect of indole-3-carboxyaldehyde, which is the starting material used for the synthesis of the inhibitor IMBH. These SEM images reveal the impact of indole-3-carboxyaldehyde on the corrosion behavior of mild steel. The presence of indole-3-carboxyaldehyde in the corrosive solution results in a noticeable reduction in the corrosion rate compared to the untreated sample. This indicates that indole-3-carboxyaldehyde exhibits corrosion inhibitory properties, and its inclusion in the inhibitor synthesis process contributes to the overall effectiveness of the final inhibitor IMBH.

The adsorption of the inhibitor molecules on the mild steel surface is a crucial factor contributing to the corrosion inhibition process. The formation of a protective adsorption layer effectively limits the interaction between the metal surface and the aggressive hydrochloric acid medium, leading to a decrease in the corrosion rate.

These surface analysis results provide compelling evidence of the corrosion inhibition mechanism achieved through the use of the tested inhibitor, IMBH and its precursor, indole-3-carboxyaldehyde. The observed alteration in the mild steel surface morphology confirms the successful formation of the protective adsorption layer, validating the inhibitors efficacy in hindering corrosion. These findings support the use of IMBH as a promising corrosion control agent, highlighting its potential for practical applications in various industrial settings. The study of indole-3-carboxyaldehyde also offers valuable insights into its role in enhancing the inhibitory performance of the synthesized inhibitor, further emphasizing its significance in the corrosion inhibition process.

The results of the EDX analysis are presented in Figure 8, and the elemental composition of the mild steel surface is summarized in Table 3 for both the presence and absence of inhibitors. Figure 8 displays the EDX spectra:

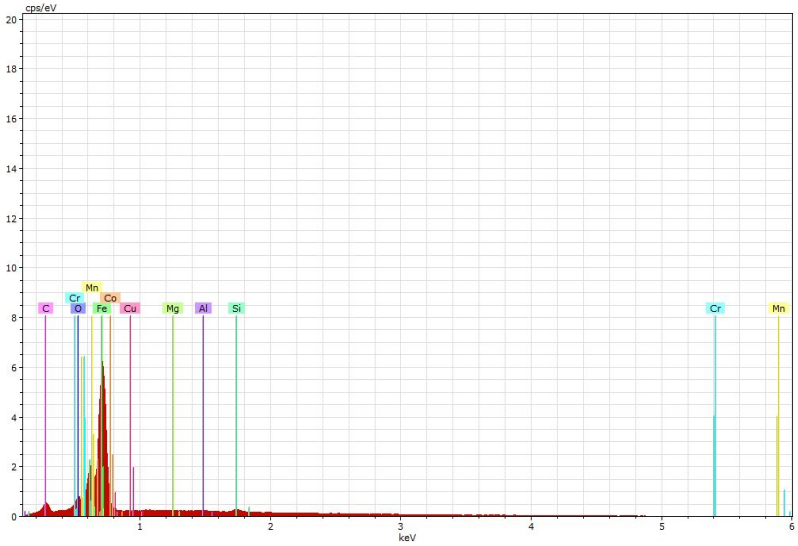

(A)

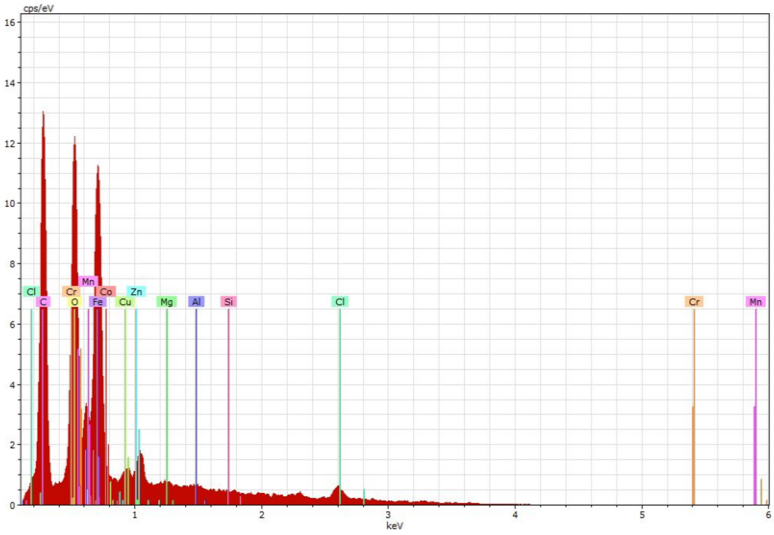

(B)

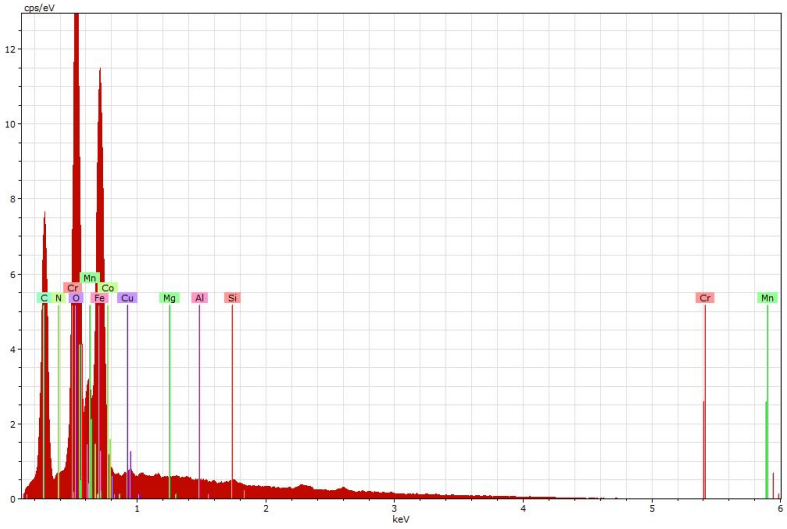

(C)

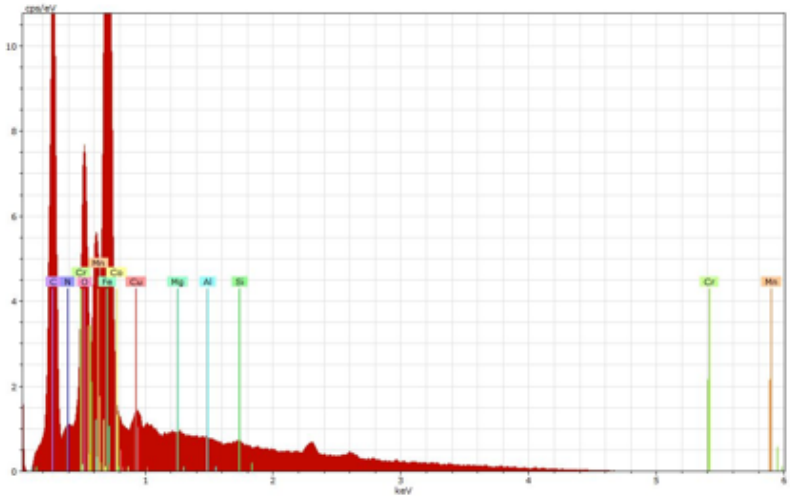

(D)

Figure 8. EDX spectra of mild steel surface. (A) polished surface, (B) after immersion in 0.2 M HCl, (C) after immersion in 0.2 M HCl, 0.005 M of indole-3-carboxyaldehyde, (D) after immersion in 0.2 M HCl, 0.005 M of IMBH.

The EDX analysis provides valuable insights into the elemental composition of the mild steel surface, shedding light on the impact of the inhibitors, indole-3-carboxyaldehyde and IMBH, on the surface properties. Table 3 presents the EDX results for mild steel, indole-3-carboxyaldehyde and IMBH.

Table 3. EDX results for Mild steel, indole-3-carboxyaldehyde, and IMBH.

Inhibitors	Fe	Cl	C	N
Mild steel	53.02	1.84	16.77	–
Indole-3-carboxyaldehyde	60.24	–	9.79	0.28
IMBH	65.18	–	13.68	0.76

The EDX results reveal notable changes in the elemental composition of the mild steel surface upon the addition of the inhibitors. In the presence of the inhibitors, there is a clear decrease in the percentage of chlorine (Cl) detected on the mild steel surface. This decrease in Cl content indicates that the inhibitors have effectively reduced the corrosive attack on the mild steel surface, leading to a decline in the formation of chlorides, which are indicative of corrosion products. Moreover, there is a substantial increase in the percentage of Fe on the mild steel surface in the presence of the inhibitors. This increase in Fe content suggests that the inhibitors have formed a protective layer that covers the mild steel surface. The formation of this protective layer, composed of inhibitor molecules, hinders the direct contact of the metal surface with the aggressive corrosive medium (HCl), leading to a decrease in the overall corrosion rate. For indole-3-carboxyaldehyde, it is evident from the EDX results that it contributes to the formation of the protective layer on the mild steel surface, as indicated by the changes in the elemental composition. However, the synthesized inhibitor IMBH exhibits even more pronounced effects, with a higher increase in Fe content and a notable reduction in Cl content compared to indole-3-carboxyaldehyde. This demonstrates the superior performance of IMBH as a corrosion inhibitor and highlights its potential for efficient corrosion control. The EDX analysis corroborates the findings from the surface analysis, confirming the successful formation of the protective adsorption layer of the inhibitors on the mild steel surface. The presence of the protective layer effectively mitigates the corrosion process, making IMBH a promising candidate for practical applications as a corrosion control agent in various industrial sectors.

The calculation method

All theoretical calculations of the compounds included in the study were performed using the Gaussian 09, version D.01 software and Becke's three-parameter hybrid (B3) exchange functional and the Lee–Yang–Parr (LYP) correlation functional (B3LYP). All geometry optimizations, the highest occupied molecular orbital energies (E_{HOMO}), and the lowest unoccupied molecular orbital energies (E_{LUMO}) are computed using a variation of the density functional theory (DFT) method using the basis set 6-311G [32, 33, 52–59]. Assist in the assessment of other important values, including ΔE, η, σ, χ, and ΔN using Equations (3–9).

$$\Delta E = E_{LUMO} - E_{HOMO} \quad (3)$$

$$\eta = -\frac{1}{2}\left(E_{\mathrm{HOMO}} - E_{\mathrm{LUMO}}\right) \quad (4)$$

$$\sigma = -\frac{1}{\eta} \quad (5)$$

$$\chi = -\frac{1}{2}\left(E_{\mathrm{HOMO}} + E_{\mathrm{LUMO}}\right) \quad (6)$$

$$\Delta N = \frac{\chi_{\mathrm{Fe}} - \chi_{\mathrm{inh}}}{2\left(\eta_{\mathrm{Fe}} + \eta_{\mathrm{inh}}\right)} \quad (7)$$

$$I = -E_{\mathrm{HOMO}} \quad (8)$$

$$A = -E_{\mathrm{LUMO}} \quad (9)$$

Mulliken charges

Mulliken charges are crucial for assessing the adsorption centers of the compounds under investigation. The examined compounds capacity to adsorb on the surface of the MS is explained by a large negative charge. In the molecules indole and IMBH, nitrogen, oxygen, and certain carbon atoms have larger negative charges, indicating coordinating bonds with the metal as seen in Figure 9. As a result, nitrogen atoms served as the active centers, which may coordinate with MS's surface [60–67]. The positive charges on the carbon atoms in this molecule, which are frequently sites where nucleophiles may bond, allow it to receive electrons from metal. A recent study found that superior inhibitors can exchange and receive electrons with the metal.

Table 4. Thermodynamic and electronic properties of compounds using DFT-B3LYP/6.311G.

Parameters	**Indole**	**IMBH**
Total energy (a.u.)	–776.9990	–856.9572
E_{HOMO} (eV)	–6.7092	–5.9538
E_{LUMO} (eV)	–1.5080	–1.6432
ΔE (eV)	5.2012	4.3106
Global hardness η	2.6006	2.1553
Chemical softness	0.3845	0.4639
Electronegativity χ	4.1086	3.7985
Fraction of electrons transferred ΔN	0.556	0.7427
Dipole moment (Debye)	3.7138	4.3670
Electron affinity (A)	1.5080	1.6432
lonization potential (I)	6.7092	5.9538

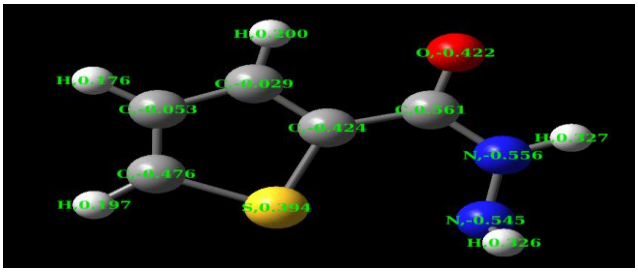

Indole

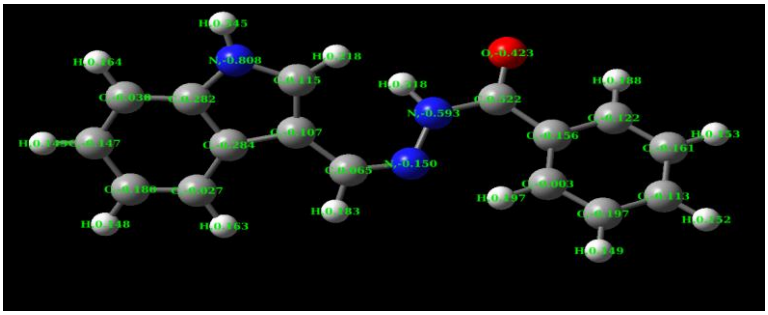

IMBH

Figure 9. Mulliken charges of indole and IMBH molecules.

Studies of quantum chemistry

Quantum chemical calculations provide valuable insights into the inhibition phenomena, allowing a deeper understanding of the inhibitory activation of the investigated inhibitor molecules, specifically indole and IMBH. Theoretical elements, such as HOMO (Highest Occupied Molecular Orbital), LUMO (Lowest Unoccupied Molecular Orbital), ΔE (energy gap), η (hardness), σ (softness), χ (electron affinity), and ΔN (fractional number of electrons transferred), play crucial roles in elucidating the nature of interactions between the metal surface and the inhibitor molecules [5]. In the current work, all the relevant quantum parameters for both indole and IMBH molecules were computed, providing quantitative insights into their inhibitory properties. Figure 10 displays the optimized structure of IMBH, allowing for an evaluation of its inhibitor efficiency based on HOMO and LUMO energies [18]. The HOMO energy value indicates the willingness of the inhibitor to donate electrons. High HOMO values suggest strong affinities of the inhibitor compounds to transfer electrons to suitable acceptor molecules. On the other hand, the LUMO energy values reflect the capability of the alloy to accept electrons from the inhibitor molecules [68, 69]. Low LUMO values indicate that the inhibitor can easily back-donate electrons from the alloy surface, further contributing to the inhibition process.

The energy gap (ΔE), calculated as the difference between E_{LUMO} and E_{HOMO}, represents the molecules inhibitive efficiency. Smaller ΔE values indicate remarkable inhibitory performance, as per the hardness and softness concept. A molecule with high hardness has low basicity and a limited ability to donate electrons, while a molecule with high softness

possesses high basicity and a strong tendency to donate electrons. The study confirms that inhibition efficacy decreases with increasing inhibitor molecule hardness and increases with decreasing softness, emphasizing the importance of inhibitor molecular properties in determining their inhibitory performance. Stability and reactivity insights are provided by hardness and softness factors, where high hardness (η) corresponds to a hard molecule with a higher electron transfer energy, and low softness (σ) implies a more efficient corrosion inhibition. The values for IMBH, as shown in Table 4, including ΔE (4.3106 eV), global softness (σ), global hardness (η), and fractional number of electrons transferred (ΔN), are consistent with the experimental results. Additionally, the calculated value of χ (3.7985), as displayed in Table 4, confirms that IMBH exhibits superior inhibitory performance due to a higher volume of electron transfers. The number of transferred electrons (N) indicates the molecule's capacity to transfer electrons to acceptor molecules, further influencing the inhibitory behavior.

The optimized molecular structure enabled the calculation of various important parameters, such as dipole moment, ionization potential (I), electron affinity (A), and the energy band gap ($E_{gap}=E_{HOMO}-E_{LUMO}$). These parameters collectively contribute to understanding the stability and interaction between the adsorbed inhibitor and the metallic substrate, represented by the energy gap (E) between HOMO and LUMO [19]. In conclusion, the quantum chemical calculations provide a comprehensive assessment of the inhibitory properties of indole and IMBH molecules. The evaluation of various quantum parameters sheds light on their electron-donating and accepting abilities, stability, and inhibitory performance. The insights gained from these calculations contribute significantly to the understanding of the inhibition mechanism and pave the way for the development of efficient corrosion control agents for practical applications in diverse industrial settings.

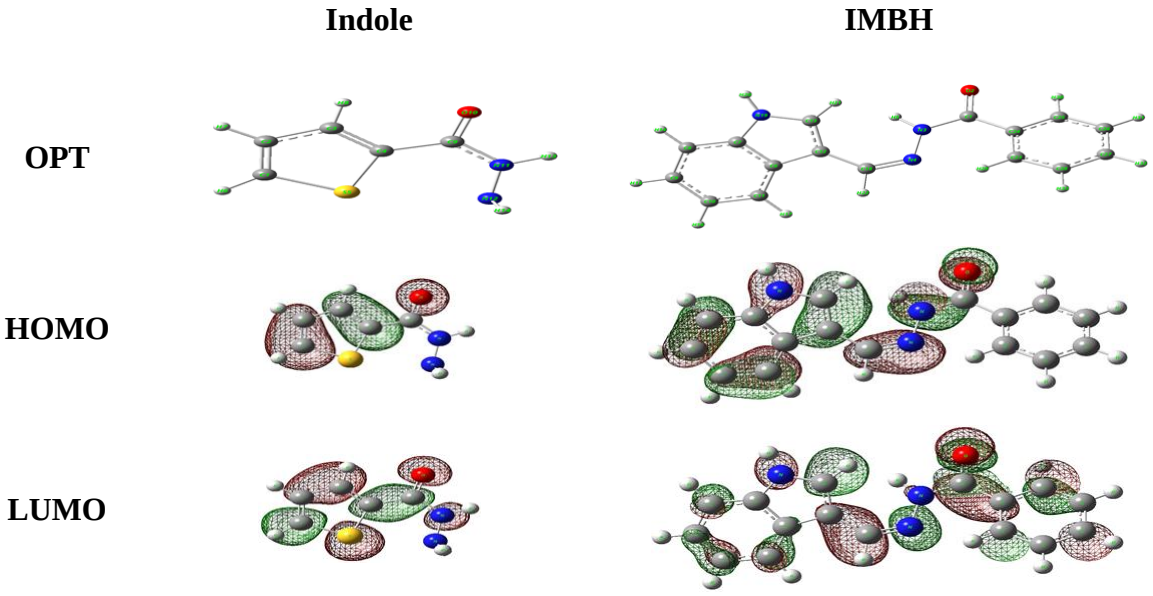

Figure 10. The geometric molecular structures and atomic contributions in the highest occupied molecular orbital HOMO and lowest unoccupied molecular orbital LUMO for Indole and IMBH were calculated using the B3LYP/6-3111G technique.

Mechanism of inhibition

The inhibition mechanism of IMBH on the corrosion of mild steel in HCl solutions (0.2 M, 0.4 M, and 0.6 M) is attributed to the adsorption of IMBH molecules at the mild steel-solution interface. The adsorption process involves a combination of physical and chemical interactions between the organic inhibitor, IMBH, and the surface of the mild steel. Physical adsorption and chemical adsorption are the two primary forms of interaction contributing to the adsorption of IMBH molecules on the mild steel surface. Physical adsorption involves weak van der Waals forces, whereas chemical adsorption involves the formation of a strong covalent bond between the inhibitor molecules and the metal surface. Several factors influence the adsorption process, thereby affecting the inhibitory efficiency of IMBH. The nature of the alloy, the chemical composition of the inhibitor molecules, the electrolyte form (HCl concentration), the environmental temperature, and the morphology of the mild steel specimen all play crucial roles in determining the extent of inhibitor adsorption and corrosion inhibition [20–23].

The alloy nature of mild steel influences the surface properties and reactivity, thereby affecting the adsorption capability of IMBH molecules. Different alloy compositions may have varying degrees of affinity for the inhibitor, leading to differences in inhibitory performance. The chemical composition of IMBH plays a crucial role in determining its adsorption characteristics. The presence of functional groups, such as –C=N– and heterocyclic structures, enables IMBH to form coordination complexes with the metal surface, contributing to the formation of a protective adsorption layer. The electrolyte form, represented by the concentration of HCl, influences the corrosive aggressiveness and the adsorption behavior of the inhibitor. Higher HCl concentrations can enhance the corrosive attack, making the adsorption of IMBH even more critical for effective corrosion protection. Environmental temperature also affects the adsorption process. Higher temperatures can lead to increased molecular mobility, facilitating adsorption of IMBH on the mild steel surface.

Furthermore, the morphology of the mild steel specimen can impact the surface area available for inhibitor adsorption. A higher surface area provides more active sites for IMBH adsorption, potentially leading to improved corrosion inhibition. In conclusion, the mechanism of inhibition of IMBH on mild steel corrosion involves the adsorption of IMBH molecules at the mild steel-solution interface. Physical and chemical adsorption interactions contribute to the formation of a protective adsorption layer on the metal surface, which effectively reduces the corrosion rate. The inhibitory efficiency is influenced by various factors, including the alloy nature, chemical composition of the inhibitor, electrolyte form, environmental temperature, and specimen morphology. Understanding the underlying mechanism is crucial for optimizing the use of IMBH as a promising corrosion control agent in diverse industrial applications. Figure 11, represents the suggested inhibition mechanism.

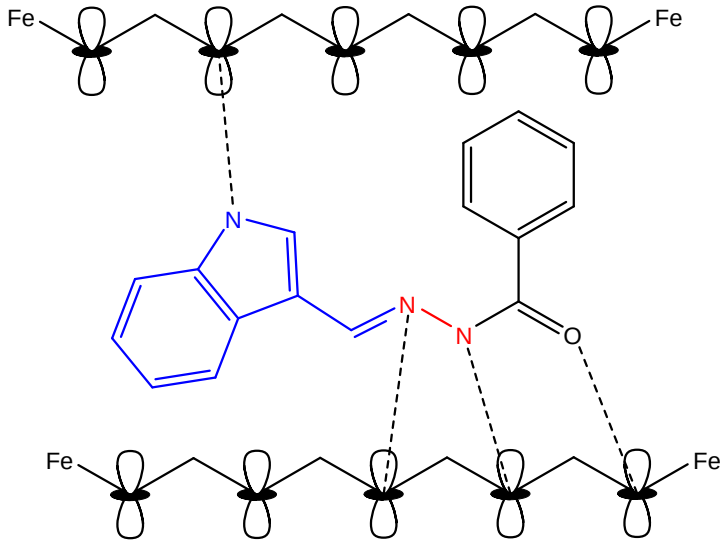

Figure 11. The suggested mechanism of inhibition of IMBH molecules.

4. Conclusion

In conclusion, this study investigated the corrosion inhibition potentials of IMBH for mild steel in HCl solutions. The synthesized IMBH and its precursor, indole-3-carboxyaldehyde, were characterized using various spectroscopic techniques, including proton nuclear magnetic resonance (^{1}H NMR), carbon-13 nuclear magnetic resonance (^{13}C NMR), and Fourier transform infrared spectroscopy (FT-IR), confirming the successful synthesis of the inhibitor.

The electrochemical studies provided valuable insights into the inhibitory performance of IMBH. Tafel measurements revealed that the addition of IMBH led to a significant decrease in the corrosion rate of mild steel in different concentrations of HCl. The inhibitory efficiency increased with rising concentrations of IMBH, demonstrating its effective protection against corrosion. The superior inhibitory performance of IMBH was attributed to the presence of –C=N– and heterocyclic groups in its molecular structure, providing additional adsorption centers on the mild steel surface. Surface analysis using SEM further confirmed the formation of a protective layer of IMBH molecules on the mild steel surface, hindering the corrosive attack and reducing the formation of corrosion products. Quantum chemical calculations provided valuable theoretical insights into the inhibition mechanism. The calculated HOMO and LUMO energies indicated the ability of IMBH to donate and accept electrons, respectively, thereby contributing to the formation of the protective adsorption layer. The low energy gap (ΔE) suggested the remarkable inhibitive efficiency of IMBH. Moreover, the values of global hardness (η), global softness (σ), and fractional number of electrons transferred (ΔN) were consistent with the experimental results, further confirming the effectiveness of IMBH as a corrosion inhibitor.

Overall, IMBH emerged as a promising corrosion inhibitor for mild steel in HCl environments. The combination of experimental studies and quantum chemical calculations provided a comprehensive understanding of its inhibitory performance and inhibition

mechanism. The presence of –C=N– and heterocyclic groups in IMBH's molecular structure played a pivotal role in enhancing its inhibitory efficiency by forming a protective adsorption layer on the mild steel surface. This research contributes to the development of efficient corrosion control strategies for industrial applications, ensuring the longevity and reliability of mild steel components in aggressive environments. Future studies can further explore the practical applicability of IMBH as a corrosion inhibitor in real-world industrial settings and investigate its performance in diverse corrosive media and under different operating conditions.

References

1. B.S. Mahdi, M.K. Abbass, M.K. Mohsin, W.K. Al-Azzawi, M.M. Hanoon, M.H.H. AlKaabi, L.M. Shaker, A.A. Al-Amiery, W.N.R.W. Isahak, A.A.H. Kadhum and M.S. Takriff, Corrosion inhibition of mild steel in hydrochloric acid environment using terephthaldehyde based on Schiff base: Gravimetric, thermodynamic, and computational studies, *Molecules*, 2022, **27**, no. 15, 4857. doi: 10.3390/molecules27154857
2. Q. Jawad, D. Zinad, R.D. Salim, A.A. Al-Amiery, T.S. Gaaz, M.S. Takriff and A. Kadhum, Synthesis, Characterization, and Corrosion Inhibition Potential of Novel Thiosemicarbazone on Mild Steel in Sulfuric Acid Environment, *Coatings*, 2019, **9**, 729. doi: 10.3390/coatings9110729
3. S. Al-Baghdadi, F. Noori, W.K. Ahmed and A.A. Al-Amiery, Thiadiazole as a potential corrosion inhibitor for mild steel in 1 M HCl, *J. Adv. Electrochem*., 2016, **2**, 67–69.
4. A.M. Resen, M. Hanoon, R.D. Salim, A.A. Al-Amiery, L.M. Shaker and A.A.H. Kadhum, Gravimetrical, theoretical, and surface morphological investigations of corrosion inhibition effect of 4-(benzoimidazole-2-yl) pyridine on mild steel in hydrochloric acid, *Koroze Ochr. Mater*., 2020, **64**, 122–130. doi: 10.2478/kom-2020-0018
5. S. Junaedi, A. Al-Amiery, A. Kadihum, A. Kadhum and A. Mohamad, Inhibition effects of a synthesized novel 4-aminoantipyrine derivative on the corrosion of mild steel in hydrochloric acid solution together with quantum chemicalstudies, *Int. J. Mol. Sci*., 2013, **14**, 11915–11928. doi: 10.3390/ijms140611915
6. A. Alamiery, W.N.R.W. Isahak, H.S.S. Aljibori, H.A. Al-Asadi and A.A.H. Kadhum, Effect of the structure, immersion time and temperature on the corrosion inhibition of 4-pyrrol-1-yl-n-(2,5-dimethyl-pyrrol-1-yl)benzoylamine in 1.0 M HCl solution, *Int. J. Corros. Scale Inhib*., 2021, **10**, no. 2, 700–713. doi: 10.17675/2305-6894-2021-10-2-14
7. S. Al-Baghdadi, F. Hashim, A. Salam, T. Abed, T. Gaaz, A. Al-Amiery, A.H. Kadhum, K. Reda and W. Ahmed, Synthesis and corrosion inhibition application of NATN on mild steel surface in acidic media complemented with DFT studies, *Results Phys*., 2018, **8**, 1178–1184. doi: 10.1016/j.rinp.2018.02.007

8. W.K. Al-Azzawi, A.J.Al Adily, F.F. Sayyid, R.K. Al-Azzawi, M.H. Kzar, H.N. Jawoosh, A.A. Al-Amiery, A.A.H. Kadhum, W.N.R.W. Isahak and M.S. Takriff, Evaluation of corrosion inhibition characteristics of an N-propionanilide derivative for mild steel in 1 M HCl: Gravimetrical and computational studies, *Int. J. Corros. Scale Inhib*., 2022, **11**, no. 3, 1100–1114. doi: 10.17675/2305-6894-2022-11-3-12
9. A. Mustafa, F. Sayyid, N. Betti, M. Hanoon, A. Al-Amiery, A. Kadhum and M. Takriff, Inhibition Evaluation of 5-(4-(1H-pyrrol-1-yl)phenyl)-2-mercapto-1,3,4-oxadiazole for the Corrosion of Mild Steel in an Acid environment: Thermodynamic and DFT Aspects, *Tribologia*, 2021, **38**, 39–47. doi: 10.30678/fjt.105330
10. Y.M. Abdulsahib, A.J.M. Eltmimi, S.A. Alhabeeb, M.M. Hanoon, A.A. Al-Amiery, T. Allami and A.A.H. Kadhum, Experimental and theoretical investigations on the inhibition efficiency of *N*-(2,4-dihydroxytolueneylidene)-4-methylpyridin-2-amine for the corrosion of mild steel in hydrochloric acid, *Int. J. Corros. Scale Inhib*., 2021, **10**, no. 3, 885–899. doi: 10.17675/2305-6894-2021-10-3-3
11. A.K. Khudhair, A.M. Mustafa, M.M. Hanoon, A. Al-Amiery, L.M. Shaker, T. Gazz, A.B. Mohamad, A.H. Kadhum and M.S. Takriff, Experimental and Theoretical Investigation on the Corrosion Inhibitor Potential of N-MEH for Mild Steel in HCl, *Prog. Color, Color. Coat*., 2022, **15**, 111–122. doi: 10.30509/PCCC.2021.166815.1111
12. D.S. Zinad, R.D. Salim, N. Betti, L.M. Shaker and A.A. AL-Amiery, Comparative Investigations of the Corrosion Inhibition Efficiency of a 1-phenyl-2-(1-phenylethylidene)hydrazine and its Analog Against Mild Steel Corrosion in Hydrochloric Acid Solution, *Prog. Color, Color. Coat*., 2022, **15**, 53–63. doi: 10.30509/pccc.2021.166786.1108
13. R.D. Salim, N. Betti, M. Hanoon and A.A. Al-Amiery, 2-(2,4-Dimethoxybenzylidene)-*N*-Phenylhydrazinecarbothioamide as an Efficient Corrosion Inhibitor for Mild Steel in Acidic Environment, *Prog. Color, Color. Coat*., 2021, **15**, 45–52. doi: 10.30509/pccc.2021.166775.1105
14. A.A. Al-Amiery, L.M. Shaker, A.H. Kadhum and M.S. Takriff, Exploration of furan derivative for application as corrosion inhibitor for mild steel in hydrochloric acid solution: Effect of immersion time and temperature on efficiency, *Mater. Today: Proc*., 2021, **42**, 2968–2973. doi: 10.1016/j.matpr.2020.12.807
15. A.M. Resen, M.M. Hanoon, W.K. Alani, A. Kadhim, A.A. Mohammed, T.S. Gaaz, A.A.H. Kadhum, A.A. Al-Amiery and M.S. Takriff, Exploration of 8-piperazine-1-ylmethylumbelliferone for application as a corrosion inhibitor for mild steel in hydrochloric acid solution, *Int. J. Corros. Scale Inhib*., 2021, **10**, no. 1, 368–387. doi: 10.17675/2305-6894-2021-10-1-21
16. M.M. Hanoon, A.M. Resen, A.A. Al-Amiery, A.A.H. Kadhum and M.S. Takriff, Theoretical and Experimental Studies on the Corrosion Inhibition Potentials of 2-((6-Methyl-2-Ketoquinolin-3-yl)Methylene) Hydrazinecarbothioamide for Mild Steel in 1 M HCl, *Prog. Color, Color. Coat*., 2021, **15**, 21–33. doi: 10.30509/PCCC.2020.166739.1095

17. F.G. Hashim, T.A. Salman, S.B. Al-Baghdadi, T. Gaaz and A.A. Al-Amiery, Inhibition effect of hydrazine-derived coumarin on a mild steel surface in hydrochloric acid, *Tribologia*, 2020, **37**, 45–53. doi: 10.30678/fjt.95510
18. A. Alamiery, L.M. Shaker, T. Allami, A.H. Kadhum and M.S. Takriff, A study of acidic corrosion behavior of Furan-Derived Schiff base for mild steel in hydrochloric acid environment: Experimental, and surface investigation, *Mater. Today: Proc*., 2021, **44**, 2337–2341. doi: 10.1016/j.matpr.2020.12.431
19. S. Al-Baghdadi, A. Al-Amiery, T. Gaaz and A. Kadhum, Terephthalohydrazide and isophthalo-hydrazide as new corrosion inhibitors for mild steel in hydrochloric acid: Experimental and theoretical approaches, *Koroze Ochr. Mater*., 2021, **65**, 12–22. doi: 10.2478/kom-2021-0002
20. M.M. Hanoon, A.M. Resen, L.M. Shaker, A. Kadhum and A. Al-Amiery, Corrosion investigation of mild steel in aqueous hydrochloric acid environment using *n*-(Naphthalen-1yl)-1-(4-pyridinyl)methanimine complemented with antibacterial studies, *Biointerface Res. Appl. Chem*., 2021, **11**, 9735–9743. doi: 10.33263/BRIAC112.97359743
21. H. Rahmani, F. El-Hajjaji, A. El Hallaoui, M. Taleb, Z. Rais, M. El Azzouzi, B. Labriti, K. Ismaily Alaoui and B. Hammouti, Experimental, quantum chemical studies of oxazole derivatives as corrosion inhibitors on mild steel in molar hydrochloric acid medium, *Int. J. Corros. Scale Inhib*., 2018, **7**, no. 4, 509–527. doi: 10.17675/2305-6894-2018-7-4-3
22. Ya.G. Avdeev, Nitrogen-containing six-membered heterocyclic compounds as corrosion inhibitors for metals in solutions of mineral acids – A review, *Int. J. Corros. Scale Inhib*., 2018, **7**, no. 4, 460–497. doi: 10.17675/2305-6894-2018-7-4-1
23. E. Barmatov and H. Trevor, Degradation of a schiff-base corrosion inhibitor by hydrolysis, and its effects on the inhibition efficiency for steel in hydrochloric acid, *Mater. Chem. Phys*., 2021, **257**, 123758.
24. F. Afshari, E.R. Ghomi, M. Dinari and S. Ramakrishna, Recent advances on the corrosion inhibition behavior of schiff base compounds on mild steel in acidic media, *ChemistrySelect*, 2023, **8**, no. 9, e202203231. doi: 10.1002/slct.202203231
25. S. Varvara, C. Berghian-Grosan, G. Damian, M. Popa and F. Popa, Combined Electrochemical, Raman Analysis and Machine Learning Assessments of the Inhibitive Properties of an 1,3,4-Oxadiazole-2-Thiol Derivative against Carbon Steel Corrosion in HCl Solution, *Materials*, 2022, **15**, 2224. doi: 10.3390/ma15062224
26. S. Al-Baghdadi, T.S. Gaaz, A. Al-Adili, A. Al-Amiery and M. Takriff, Experimental studies on corrosion inhibition performance of acetylthiophene thiosemicarbazone for mild steel in HCl complemented with DFT investigation, *Int. J. Low-Carbon Technol*., 2021, **16**, 181–188. doi: 10.1093/ijlct/ctaa050

27. A. Al-Amiery, Anti-corrosion performance of 2-isonicotinoyl-N-phenylhydrazinecarbothioamide for mild steel hydrochloric acid solution: Insights from experimental measurements and quantum chemical calculations, *Surf. Rev. Lett*., 2021, **28**, 2050058. doi: 10.1142/S0218625X20500584
28. A.A. Alamiery, Investigations on corrosion inhibitory effect of newly quinoline derivative on mild steel in HCl solution complemented with antibacterial studies, *Biointerface Res. Appl. Chem*., 2022, **12**, 1561–1568. doi: 10.33263/BRIAC122.15611568
29. ASTM International, Standard Practice for Preparing, Cleaning and Evaluating Corrosion Test, 2011, 1–9.
30. NACE International, Laboratory Corrosion Testing of Metals in Static Chemical Cleaning Solutions at Temperatures below 93°C (200°F), TM0193-2016-SG, 2000
31. I.A. Alkadir Aziz, I.A. Annon, M.H. Abdulkareem, M.M. Hanoon, M.H. Alkaabi, L.M. Shaker, A.A. Alamiery, W.N.R. Wan Isahak and M.S. Takriff, Insights into Corrosion Inhibition Behavior of a 5-Mercapto-1, 2, 4-triazole Derivative for Mild Steel in Hydrochloric Acid Solution: Experimental and DFT Studies, *Lubricants*, 2021, **9**, 122. doi: 10.3390/lubricants9120122
32. M.J. Frisch, G.W. Trucks, H.B. Schlegel, G.E. Scuseria, M.A. Robb, J.R. Cheeseman, J.A. Montgomery, T. Vreven, K.N. Kudin, J.C. Burant, J.M. Millam, S.S. Iyengar, J. Tomasi, V. Barone, B. Mennucci, M. Cossi, G. Scalmani, N. Rega, G.A. Petersson, H. Nakatsuji, M. Hada, M. Ehara, K. Toyota, R. Fukuda, J. Hasegawa, M. Ishida, T. Nakajima, Y. Honda, O. Kitao, H. Nakai, M. Klene, X. Li, J.E. Knox, H.P. Hratchian, J.B. Cross, V. Bakken, C. Adamo, J. Jaramillo, R. Gomperts, R.E. Stratmann, O. Yazyev, A.J. Austin, R. Cammi, C. Pomelli, J.W. Ochterski, P.Y. Ayala, K. Morokuma, G.A. Voth, P. Salvador, J.J. Dannenberg, V.G. Zakrzewski, S. Dapprich, A.D. Daniels, M.C. Strain, O. Farkas, D.K. Malick, A.D. Rabuck, K. Raghavachari, J.B. Foresman, J.V. Ortiz, Q. Cui, A.G. Baboul, S. Clifford, J. Cioslowski, B.B. Stefanov, G. Liu, A. Liashenko, P. Piskorz, I. Komaromi, R.L. Martin, D.J. Fox, T. Keith, M.A. Al-Laham, C.Y. Peng, A. Nanayakkara, M. Challacombe, P.M.W. Gill, B. Johnson, W. Chen, M.W. Wong, C. Gonzalez and J.A. Pople, Gaussian 03, Revision B. 05, *Gaussian, Inc*., Wallingford, CT, 2004.
33. T. Koopmans, Ordering of wave functions and eigen-energies to the individual electrons of an atom, *Physica*, 1934, **1**, no. 1–6, 104–113 (in German). doi: 10.1016/S0031-8914(34)90011-2
34. A. Alamiery, Short report of mild steel corrosion in 0.5 M H_2SO_4 by 4-ethyl-1-(4-oxo4-phenylbutanoyl)thiosemicarbazide, *Tribologia*, 2021, **30**, 90–99.
35. A.A. Alamiery, W.N.R.W. Isahak and M.S. Takriff, Inhibition of mild steel corrosion by 4-benzyl-1-(4-oxo-4-phenylbutanoyl)thiosemicarbazide: Gravimetrical, adsorption and theoretical studies, *Lubricants*, 2021, **9**, 93. doi: 10.3390/lubricants9090093

36. M.A. Dawood, Z.M.K. Alasady, M.S. Abdulazeez, D.S. Ahmed, G.M. Sulaiman, A.A.H. Kadhum, L.M. Shaker and A.A. Alamiery, The corrosion inhibition effect of a pyridine derivative for low carbon steel in 1 M HCl medium: Complemented with antibacterial studies, *Int. J. Corros. Scale Inhib*., 2021, **10**, no. 4, 1766–1782. doi: 10.17675/2305-6894-2021-10-4-25
37. A. Alamiery, Corrosion inhibition effect of 2-*N*-phenylamino-5-(3-phenyl-3-oxo-1-propyl)-1,3,4-oxadiazole on mild steel in 1 M hydrochloric acid medium: Insight from gravimetric and DFT investigations, *Mater. Sci. Energy Technol*., 2021, **4**, 398–406. doi: 10.1016/j.mset.2021.09.002
38. A. Alamiery, Anticorrosion effect of thiosemicarbazide derivative on mild steel in 1 M hydrochloric acid and 0.5 M sulfuric Acid: Gravimetrical and theoretical studies, *Mater. Sci. Energy Technol*., 2021, **4**, 263–273. doi: 10.1016/j.mset.2021.07.004
39. A. Alamiery, W.N.R.W. Isahak, H. Aljibori, H. Al-Asadi and A. Kadhum, Effect of the structure, immersion time and temperature on the corrosion inhibition of 4-pyrrol-1-yln-(2,5-dimethyl-pyrrol-1-yl)benzoylamine in 1.0 M HCl solution, *Int. J. Corros. Scale Inhib*., 2021, **10**, no. 2, 700–713. doi: 10.17675/2305-6894-2021-10-2-14
40. A. Alamiery, E. Mahmoudi and T. Allami, Corrosion inhibition of low-carbon steel in hydrochloric acid environment using a Schiff base derived from pyrrole: gravimetric and computational studies, *Int. J. Corros. Scale Inhib*., 2021, **10**, no. 2, 749–765. doi: 10.17675/2305-6894-2021-10-2-17
41. A.J.M. Eltmimi, A. Alamiery, A.J. Allami, R.M. Yusop, A.H. Kadhum and T. Allami, Inhibitive effects of a novel efficient Schiff base on mild steel in hydrochloric acid environment, *Int. J. Corros. Scale Inhib*., 2021, **10**, no. 2, 634–648. doi: 10.17675/2305-6894- 2021-10-2-10
42. A. Döner, R. Solmaz, M. Özcan and G. Kardaş, Experimental and theoretical studies of thiazoles as corrosion inhibitors for mild steel in sulphuric acid solution, *Corros. Sci*., 2011, **53**, no. 9, 2902–2913. doi: 10.1016/j.corsci.2011.05.027
43. M.S. Abdulazeez, Z.S. Abdullahe, M.A. Dawood, Z.K. Handel, R.I. Mahmood, S. Osamah, A.H. Kadhum, L.M. Shaker and A.A. Al-Amiery, Corrosion inhibition of low carbon steel in HCl medium using a thiadiazole derivative: weight loss, DFT studies and antibacterial studies, *Int. J. Corros. Scale Inhib*., 2021, **10**, no. 4, 1812–1828. doi: 10.17675/2305-6894-2021-10-4-27
44. A.Z. Salman, Q.A. Jawad, K.S. Ridah, L.M. Shaker and A.A. Al-Amiery, Selected BISThiadiazole: Synthesis and Corrosion Inhibition Studies on Mild Steel in HCL Environment, *Surf. Rev. Lett*., 2020, **27**, 2050014. doi: 10.1142/S0218625X20500146
45. S. Al-Bghdadi, M. Hanoon, J. Odah, L. Shaker and A. Al-Amiery, Benzylidene as Efficient Corrosion Inhibition of Mild Steel in Acidic Solution, *Proceedings*, 2019, **41**, 27. doi: 10.3390/ecsoc-23-06472

46. B.S. Mahdi, H.S.S. Aljibori, M.K. Abbass, W.K. Al-Azzawi, A.H. Kadhum, M.M. Hanoon, W.N.R.W. Isahak, A.A. Al-Amiery and H.Sh. Majdi, Gravimetric analysis and quantum chemical assessment of 4-aminoantipyrine derivatives as corrosion inhibitors, *Int. J. Corros. Scale Inhib*., 2022, **11**, no. 3, 1191–1213. doi: 10.17675/2305-6894-2022-11-3-17
47. A.A. Alamiery, Study of Corrosion Behavior of *N′*-(2-(2-oxomethylpyrrol-1-yl) ethyl) piperidine for Mild Steel in the Acid Environment, *Biointerface Res. Appl. Chem*., 2022, **12**, 3638–3646. doi: 10.33263/BRIAC123.36383646
48. A. Alamiery, A. Mohamad, A. Kadhum and M. Takriff, Comparative data on corrosion protection of mild steel in HCl using two new thiazoles, *Data Brief*, 2022, **40**, 107838. doi: 10.1016/j.dib.2022.107838
49. A.M. Mustafa, F.F. Sayyid, N. Betti, L.M. Shaker, M.M. Hanoon, A.A. Alamiery, A.A.H. Kadhum and M.S. Takriff, Inhibition of mild steel corrosion in hydrochloric acid environment by 1-amino-2-mercapto-5-(4-(pyrrol-1-yl)phenyl)-1,3,4-triazole, *S. Afr. J. Chem. Eng*., 2022, **39**, 42–51. doi: 10.1016/j.sajce.2021.11.009
50. A. Singh, E. Ebenso, M. Quraishi, Adsorption Behaviour of Cefapirin on Mild Steel in Hydrochloric Acid Solution, *Int. J. Electrochem. Sci*., 2012, **7**, 2320–2330.
51. A. Singh and M. Quraishi, The Effect of Some Bis-Thiadiazole Derivatives on the Corrosion of Mild Steel in Hydrochloric Acid, *Corros. Sci*., 2010, **52**, 1373–1385, doi: 10.1016/j.corsci.2010.01.007
52. M. Hegazy, A. Hasan, M. Emara, M. Bakr and A. Youssef, Evaluating Four Synthesized Schiff Bases as Corrosion Inhibitors on the Carbon Steel in 1 M Hydrochloric Acid., *Corros. Sci*., 2012, **65**, 67–76, doi: 10.1016/j.corsci.2012.08.005
53. M. Yadav, S. Kumar, R. Sinha and S. Kumar, Experimental and Theoretical Studies on Synthesized Compounds as Corrosion Inhibitor for Mild Steel in Hydrochloric Acid Solution, *J. Dispersion Sci. Technol*., 2014, **35**, 1751–1763, doi: 10.1080/01932691.2013.879831
54. A. Singh, A. Pandey, P. Banerjee, S. Saha, B. Chugh, S. Thakur, B. Pani, P. Chaubey and G. Singh, Eco-Friendly Disposal of Expired Anti-Tuberculosis Drug Isoniazid and Its Role in the Protection of Metal, *J. Environ. Chem. Eng*., 2019, **7**, 102971. doi: 10.1016/j.jece.2019.102971
55. M. Benabdellah, A. Tounsi, K. Khaled and B. Hammouti, Thermodynamic, Chemical and Electrochemical Investigations of 2-Mercapto Benzimidazole as Corrosion Inhibitor for Mild Steel in Hydrochloric Acid Solutions, *Arabian J. Chem*., 2011, **4**, 17–24. doi: 10.1016/j.arabjc.2010.06.010
56. R. Haldhar, D. Prasad, A. Saxena and P. Singh, Valeriana Wallichii Root Extract as a Green & Sustainable Corrosion Inhibitor for Mild Steel in Acidic Environments: Experimental and Theoretical, *Mater. Chem. Front*., 2018, **2**, 1225–1237. doi: 10.1039/C8QM00120K
57. A.K. Singh, S. Shukla and E. Ebenso, Cefacetrile as Corrosion Inhibitor for Mild Steel in Acidic Media, *Int. J. Electrochem. Sci*., 2011, **6**, 5689–5700.

58. W.K. Al-Azzawi, S.M. Salih, A.F. Hamood, R.K. Al-Azzawi, M.H. Kzar, H.N. Jawoosh, L.M. Shakier, A. Al-Amiery, A.A.H. Kadhum, W.N.R.W. Isahak and M.S. Takriff, Adsorption and theoretical investigations of a Schiff base for corrosion inhibition of mild steel in an acidic environment, *Int. J. Corros. Scale Inhib*., 2022, **11**, no. 3, 1063–1082. doi: 10.17675/2305-6894-2022-11-3-10
59. D.M. Jamil, A. Al-Okbi, M. Hanon, K.S. Rida, A. Alkaim, A. Al-Amiery, A. Kadhum and A.A.H. Kadhum, Carbethoxythiazole corrosion inhibitor: as an experimentally model and DFT theory, *J. Eng. Appl. Sci*., 2018, **13**, 3952–3959. doi: 10.3923/JEASCI.2018.3952.3959
60. A. Alobaidy, A. Kadhum, S. Al-Baghdadi, A. Al-Amiery, A. Kadhum, E. Yousif and A.B. Mohamad, Eco-friendly corrosion inhibitor: experimental studies on the corrosion inhibition performance of creatinine for mild steel in HCl complemented with quantum chemical calculations, *Int. J. Electrochem. Sci*., 2015, **10**, 3961–3972. doi: 10.1016/S1452-3981(23)06594-X
61. A. Al-Amiery, L.M. Shaker, A.A.H. Kadhum and M.S. Takriff, Synthesis, characterization and gravimetric studies of novel triazole-based compound, *Int. J. Low Carbon Technol*., 2020, **15**, no. 2, 164–170. doi: 10.1093/ijlct/ctz067
62. S. Junaedi, A.A.H. Kadhum, A. Al-Amiery, A.B. Mohamad and M.S. Takriff, Synthesis and characterization of novel corrosion inhibitor derived from oleic acid: 2-Amino-5-Oleyl 1,3,4-Thiadiazol (AOT), *Int. J. Electrochem. Sci*., 2012, **7**, 3543–3554. doi: 10.1016/S1452-3981(23)13976-9
63. H. Ibraheem, Y. Al-Majedy and A. Al-Amiery, 4-Thiadiazole: The Biological Activities, *Sys. Rev. Pharm*., 2018, **9**, no. 1, 36–40. doi: 10.5530/srp.2018.1.7
64. A. Al-Amiery, Y. Al-Majedy, D. Al-Duhaidahawi, A. Kadhum and A. Mohamad, Green Antioxidants: Synthesis and Scavenging Activity of Coumarin Thiadiazoles as Potential Antioxidants Complemented by Molecular Modeling Studies, *Free Radicals Antioxid*., 2016, **6**, no. 2, 173–177. doi: 10.5530/fra.2016.2.7
65. A. Al-Amiery, A. Al-Temimi, G. Sulaiman, A. Aday, A. Kadhum and A. Mohamad, Synthesis, Antimicrobial And Antioxidant Activities of 5-((2-Oxo-2h-Chromen-7-Yloxy)Methyl)-1,3,4-Thiadiazol-2(3h)One Derived From Umbelliferone, *Chem. Nat. Compd*., 2013, **48**, 950–954. doi: 10.1007/s10600-013-0436-0
66. I. Annon, A. Abbas, W. Al-Azzawi, M. Hanoon, A. Alamiery, W. Isahak and A. Kadhum, Corrosion inhibition of mild steel in hydrochloric acid environment using thiadiazole derivative: Weight loss, thermodynamics, adsorption and computational investigations, *S. Afr. J. Chem. Eng*., 2022, **41**, 244–252. doi: 10.1016/j.sajce.2022.06.011
67. H.S. Aljibori, A.H. Alwazir, S. Abdulhadi, W.K. Al-Azzawi, A.A.H. Kadhum, L.M. Shaker, A.A. Al-Amiery and H.Sh. Majdi, The use of a Schiff base derivative to inhibit mild steel corrosion in 1 M HCl solution: a comparison of practical and theoretical findings, *Int. J. Corros. Scale Inhib*., 2022, **11**, no. 4, 1435–1455. doi: 10.17675/2305- 6894-2022-11-4-2

68. H.S. Aljibori, O.H. Abdulzahra, A.J.Al Adily, W.K. Al-Azzawi, A.A. Al-Amiery and A.A.H. Kadhum, Recent progresses in thiadiazole derivatives as corrosion inhibitors in hydrochloric acid solution, *Int. J. Corros. Scale Inhib*., 2023, **12**, no. 3, 842–866. doi: 10.17675/2305-6894-2023-12-3-3
69. L.M. Shaker, A. Alamiery, W.N.R.W. Isahak and W.K. Al-Azzawi, Corrosion in solar cells: challenges and solutions for enhanced performance and durability, *J. Opt*., 2023. doi: 10.1007/s12596-023-01277-9

♦ ♦ ♦